ACS APPLIED MATERIALS & INTERFACES

Research Article

www.acsami.org

Assessing the Potential Roles of Silicon and Germanium Phthalocyanines in Planar Heterojunction Organic Photovoltaic Devices and How Pentafluoro Phenoxylation Can Enhance $\pi-\pi$ Interactions and Device Performance

Benoît H. Lessard,[†] Robin T. White,[‡] Mohammad AL-Amar,[†] Trevor Plint,[†] Jeffrey S. Castrucci,[†,‡] David S. Josey,[†] Zheng-Hong Lu,[‡] and Timothy P. Bender*[,†,‡,§]

[†]Department of Chemical Engineering and Applied Chemistry, University of Toronto, 200 College Street, Toronto, Ontario M5S 3E5, Canada

[‡]Department of Materials Science and Engineering, University of Toronto, 184 College Street, Toronto, Ontario M5S 3E4, Canada

[§]Department of Chemistry, University of Toronto, 80 St. George Street, Toronto, Ontario M5S 3H6, Canada

Supporting Information

ABSTRACT: In this study, we have assessed the potential application of dichloro silicon phthalocyanine (Cl_2-SiPc) and dichloro germanium phthalocyanine (Cl_2-GePc) in modern planar heterojunction organic photovoltaic (PHJ OPV) devices. We have determined that Cl_2-SiPc can act as an electron donating material when paired with C_{60} and that Cl_2-SiPc or Cl_2-GePc can also act as an electron acceptor material when paired with pentacene. These two materials enabled the harvesting of triplet energy resulting from the singlet fission process in pentacene. However, contributions to the generation of photocurrent were observed for Cl_2-SiPc with no evidence of photocurrent contribution from Cl_2-GePc. The result of our initial assessment established the potential for the application of SiPc and GePc in PHJ OPV devices. Thereafter, bis(pentafluoro phenoxy) silicon phthalocyanine (F_{10}-SiPc) and bis(pentafluoro phenoxy) germanium phthalocyanine (F_{10}-GePc) were synthesized and characterized. During thermal processing, it was discovered that F_{10}-SiPc and F_{10}-GePc underwent a reaction forming small amounts of difluoro SiPc (F_2-SiPc) and difluoro GePc (F_2-GePc). This undesirable reaction could be circumvented for F_{10}-SiPc but not for F_{10}-GePc. Using single crystal X-ray diffraction, it was determined that F_{10}-SiPc has significantly enhanced $\pi-\pi$ interactions compared with that of Cl_2-SiPc, which had little to none. Unoptimized PHJ OPV devices based on F_{10}-SiPc were fabricated and directly compared to those constructed from Cl_2-SiPc, and in all cases, PHJ OPV devices based on F_{10}-SiPc had significantly improved device characteristics compared to Cl_2-SiPc.

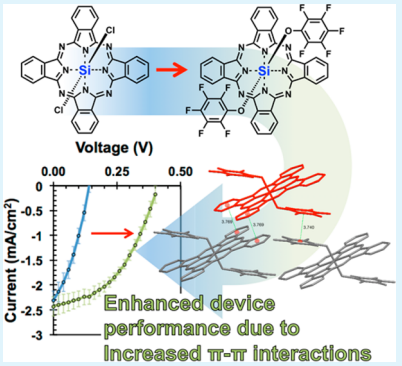

KEYWORDS: *silicon, germanium, phthalocyanine, fullerene, photovoltaic, solar, pentacene, fluorophenoxy*

INTRODUCTION

Metal containing phthalocyanines (MPcs) are planar, four membered aromatic macrocycles, which chelate a single metal atom within their internal cavity. Depending on the included metal, MPcs can be inexpensive to manufacture and relatively versatile, having applications in numerous commercial products such as dyes and pigments.[1−6] MPcs also have been applied as active components in organic electronic devices due to their charge transport and optophysical properties. For example, MPcs have been utilized as active/semiconducting layers in organic thin film transistors (OTFTs),[7−9] organic light emitting diodes (OLEDs)[10−12] and organic photovoltaic (OPV) devices.[13−15]

Divalent MPcs are arguably the most studied. For example, zinc phthalocyanine (ZnPc) and copper phthalocyanine (CuPc) are widely studied and have found application in OTFTs,[8] organic sensors,[16] OPV devices[17,18] and other organic electronics. To a lesser extent, trivalent MPcs such as chloro aluminum Pc (Cl-AlPc),[19,20] chloro gallium Pc (Cl-GaPc)[21] and even chloro indium Pc (Cl-InPc)[19,21,22] have also found application in organic electronic devices such as OPV devices. However, the use of tetravalent metal and metalloid containing Pcs in organic electronic devices is rare. The presence of a tetravalent metal/metalloid such as silicon or germanium results in a Pc with two axial bonds available for chemical reaction perpendicular to the Pc plane. Axial groups/molecular fragments can be two halogens, hydroxyl groups or even phenoxy groups.

Our group has been interested in the application of boron subphthalocyanine (BsubPc) in OPV devices and OLEDs for several years,[23,24] as have other groups (primarily in OPV devices).[25−29] The prototypical BsubPc derivative is chloro

Received: June 18, 2014
Accepted: February 9, 2015
Published: February 9, 2015

DOI: 10.1021/am508491v
ACS Appl. Mater. Interfaces 2015, 7, 5076−5088

boron subphthalocyanine (Cl-BsubPc).[30] We have recently become interested in exploring alternative metalloid Pcs in the same area of the periodic table as boron and assessing their potential for application in organic electronic devices.

In the early 1980s, Loutfy and co-workers explored the use of dichloro silicon and dichloro germanium phthalocyanines (Cl_2-SiPc and Cl_2-GePc, respectively, Figure 1) and their respective dihydroxy-MPc derivatives in a single active layer OPV devices.[31] Although the cell characteristics were poor by modern standards, their results did however indicate that silicon and germanium containing Pcs could potentially be used in OPV devices.[31] Thereafter, Xerox Corporation developed a patent position on the use of GePcs in xerographic organic photoreceptors.[32−36] Since then, very few examples can be found in the literature employing SiPc or GePc in an organic electronic device. Although some groups have utilized SiPc containing molecules as a photoactive dye in a dye-sensitized solar cells (DSSCs),[37] or as a ternary additive in a P3HT/$PC_{61}BM$/Dye bulk heterojunction (BHJ) ternary OPV devices,[38−40] their use as an active layer in a planar heterojunction (PHJ) organic electronic devices has not been explored.

Anthony et al. has shown that by chemical modification of pentacene a significant enhancement of the $\pi-\pi$ interactions in the solid-state arrangement can be obtained resulting in enhanced OTFT device performance.[41−43] Likewise, in our recent work involving BsubPc, we have identified that simple axial functionalization of the boron atom, such as using a pentafluoro phenoxy group, can have significant effect on solubility, solid-state arrangement, sublimation temperature, optical and even electrochemical behavior of the BsubPc.[30,44,45] However, very few examples of phenoxy derivatives of tetravalent MPcs such as silicon or germanium have been reported. There are some examples of axially substituted SiPc such as bis(tri-*n*-hexylsiloxy)(2,3-phthalocyaninato)silicon,[40,46] pyridine substituted SiPcs,[47−49] SiPc dimers,[50] dendrimer substituted SiPcs,[51−53] pyrene or thiophene substituted SiPcs[54] and even $C_{60}-SiPc-C_{60}$ triads.[55]

In this study we detail our reinvestigation of Cl_2-SiPc and Cl_2-GePc within PHJ OPV devices with a modern perspective. After our initial assessment and by examining the single crystal X-ray diffraction of Cl_2-SiPc, it becomes apparent that although the Pc unit is planar, very few $\pi-\pi$ interactions exist between the neighboring Cl_2-SiPcs.[56] Therefore, we have also synthesized and fully characterized bis(pentafluoro phenoxy) SiPc (F_{10}-SiPc) and bis(pentafluoro phenoxy) GePc (F_{10}-GePc). We noted an enhanced solid-state arrangement of the SiPc chromophore when the pentafluoro phenoxy molecular fragment was present and an enhancement of the resulting PHJ OPV characteristics compared against the precursor, Cl_2-SiPc. Finally, PHJ OPV devices were fabricated and used to evaluate the compounds compared to their respective dichloride precursors.

EXPERIMENTAL SECTION

Materials. Pentafluoro phenol (>99%) and potassium hydroxide (KOH, 85%) bathocuproine (BCP sublimed grade, 99.99% trace metals basis) were obtained from Sigma-Aldrich and chlorobenzene (99.5%) and chloroform ($CHCl_3$, 99.8%) were obtained from Caledon Laboratories Ltd. Pentacene (Lumtec, device grade) and poly(3,4-ethylenedioxythiophene) polystyrene sulfonate (PEDOT:PSS, Heraeus, Clevois P VP Al 4083) were purchased and used as received. Fullerene (SES Research, 99.5%) was purchased and purified once by train sublimation before use. Silver (Ag, 99.999%) was obtained from R.D. Mathis and used as is. All chemicals were used as received unless otherwise specified. Dichloro silicon phthalocyanine (Cl_2-SiPc),[57,58] dichloro germanium phthalocyanine (Cl_2-GePc)[59−61] and chloro aluminum phthalocyanine Cl-AlPc[62] were synthesized according to the published procedures. In all cases, the compounds we synthesized were purified by train sublimation prior to device integration. Each compound was analyzed prior to device fabrication by mass spectrometry to confirm that no peripheral chlorination was present.[63]

Bis(pentafluoro phenoxy) Silicon Phthalocyanine (F_{10}-SiPc). An oven-dried three-neck glass round-bottom flask was connected to a condenser and placed on a heating mantel while being purged with nitrogen. Prior to sealing the reactor with rubber septa, a mixture of Cl_2-SiPc (1.00 g, 1.64 mmol), pentafluoro phenol (1.01 g, 5.45 mmol), and toluene (10 mL) were added along with a Teflon stirbar. The mixture was then heated to reflux for 20 h while maintaining a nitrogen purge. The organic mixture was cooled and washed with 1 M KOH solution 3 times, and 3 times using neutral H_2O, before being dried. (Yield: 1.3 g, 87%). Prior to device fabrication, F_{10}-SiPc was purified using train sublimation[64] at 350 °C ($1-5 \times 10^{-3}$ Torr) using CO_2 as a carrier gas. ^{1}H NMR spectroscopy ($CDCl_3$, TMS): Aromatic, 8H, 9.69 ppm and 8H, 8.41 ppm. DART mass spectroscopy: calculated mass, 907.108; obtained mass, 907.107. EA: expected wt %, C (58.28%), H (1.78%) and N (12.36%); analysis wt %, C (59.10%) H (1.94%) N (13.28%). UV−vis ($CHCl_3$) λ_{max} = 686 nm.

Bis(pentafluoro phenoxy) Germanium Phthalocyanine (F_{10}-GePc). The synthesis of F_{10}-GePc was accomplished in an identical fashion to that of F_{10}-SiPc except Cl_2-GePc was used instead of Cl_2-SiPc. (Yield: 1.2 g, 65%). ^{1}H NMR spectroscopy ($CDCl_3$, TMS): Aromatic, 8H, 9.69 ppm and 8H, 8.41 ppm. DART LR mass spectroscopy: calculated mass, 951.3; obtained mass, 951.0. UV−vis ($CHCl_3$) λ_{max} = 692 nm. Purification of F_{10}-GePc was attempted using train sublimation 370 °C ($1-5 \times 10^{-3}$ Torr) using N_2 or CO_2, resulting in decomposition (see the Results and Discussion section). Therefore, no electronic-grade purity of the sample could be obtained.

Difluoro Silicon Phthalocyanine (F_2-SiPc). In a 50 mL three neck round-bottom flask with reflux condenser and nitrogen inlet, Cl_2-SiPc (0.1 g, 0.163 mmol) and cesium fluoride (0.06 g, 0.395 mmol) were dissolved in DMF (1 mL). The mixture was stirred and heated at 150 °C under nitrogen for 30 min. The crude product was allowed to cool to 130 °C and was precipitated into 150 mL of isopropyl alcohol. The final product was gravity filtered resulting in a fine dark indigo colored powder. Yield: 0.068 g (71%). UV−vis (DMSO) λ_{max} = 688 nm. HRMS [M^+]: calculated, 578.1231; found, 578.1235.

Difluoro Germanium Phthalocyanine (F_2-GePc). F_2-GePc was synthesized in a similar fashion to F_2-SiPc except Cl_2-GePc was used instead of Cl_2-SiPc. Yield: 0.076 g (69%). UV−vis (DMSO) λ_{max} = 680 nm. HRMS [M^+]: calculated, 624.0678; found, 624.0690.

Characterization. Ultraviolet−visible (UV−vis) spectroscopy was performed on a PerkinElmer Lambda 1050 in either a toluene solution using a 10 mm quartz cuvette or by using a film that was prepared by thermal evaporation onto a microscope slide. Cyclic voltammetry (CV) was performed using a three-electrode cell assembly at room temperature in a 0.1 M tetrabutylammonium perchlorate (TBAP) in dichloromethane electrolyte solution. The working electrode was a glassy carbon disk electrode, the counter electrode was a polished platinum wire and the reference electrode was Ag/AgCl. An internal standard of bis(pentamethyl cyclopentadienyl)iron ($E_{1/2,red}$ = 0.012 V) and a scan rate of 100 mV/s were used for all measurements unless specified otherwise. The samples were bubbled with nitrogen until no dissolved oxygen was present (30−60 min prior to each run). Photoemission measurements were conducted on a PHI 5500 Multitechnique system using a monochromated Al Kα photon source ($h\nu$ = 1486.7 eV) for X-ray photoemission spectroscopy (XPS) and a nonmonochromated He Iα photon source ($h\nu$ = 21.22 eV) for UPS. Work function and valence-band measurements were carried out using UPS with the sample tilted to a takeoff angle of 89° and under an applied bias of −15 V. The analysis chamber base pressure was $\approx 10^{-10}$ Torr.

Electronic Device Fabrication. Devices were fabricated on 25 mm by 25 mm glass substrates with patterned indium tin oxide (ITO)

DOI: 10.1021/am508491v
ACS Appl. Mater. Interfaces 2015, 7, 5076−5088

having a sheet resistance of 15 Ω/sq (Thin Film Devices, Inc.). Patterned ITO was used where 70% of the surface area was covered with a continuous region of ITO. Slides were cleaned by 5 min sonications in detergent in deionized water, pure deionized water, acetone and then methanol. The substrates were dried and treated with an air-plasma for 2 min followed by application of a suspension of PEDOT:PSS by spin-casting at 500 rpm for 10 s followed by 4000 rpm for 30 s. The samples were then annealed on a hot plate held at 110 °C for 10 min before transfer into a nitrogen atmosphere glovebox. The substrates were then transferred into a custom vacuum chamber via load lock and transfer arm. The vacuum chamber had a base pressure of $\sim 8 \times 10^{-8}$ Torr and a working pressure $\sim 1 \times 10^{-7}$ Torr for organic layer deposition. Layer thickness and deposition rate were monitored using a quartz crystal microbalance (QCM) calibrated against films deposited on glass with thicknesses measured by step edge contact profilometry. All subsequent device layers were deposited in the vacuum chamber by physical vapor deposition with a shadow mask that was manually changed by transfer into glovebox between the deposition of the BCP and Ag layers. OPV devices of dimensions 2 × 10 mm (20 mm^2) were formed from the overlap of the electrode and the ITO region.

Electronic Device Characterization. The OPV devices were transferred directly from the vacuum chamber back to the nitrogen glovebox and tested in the glovebox. Silver paste (PELCO Conductive Silver 187) was applied to the electrode end and ITO contact point to enhance electrical contact and left to cure for 30 min before testing. Simulated solar light was supplied by a 300 W xenon arc lamp with an Air Mass 1.5 Global filter, fed through a Cornerstone 260 1/4 m monochromator and then into the glovebox by way of a single branch liquid light guide. Light intensity was calibrated with reference to a UV-silicon photodetector. Voltage sweeps of the devices were performed under full spectrum illumination, and corresponding currents were measured with a Keithley 2401 Low Voltage SourceMeter, controlled by a custom LabView program. Wavelength scans of the devices were performed and corresponding currents measured using a Newport Optical Power Meter 2936-R controlled by TracQ Basic software. External quantum efficiencies were calculated using a reference wavelength scan of the UV-silicon photodetector.

RESULTS AND DISCUSSION

As a point of reference for this study we choose Cl-AlPc in place of Cl-BsubPc. Although aluminum is not a metalloid, we decided to choose Cl-AlPc due to the structural similarly of the phthalocyanine ligand to that of Cl_2-SiPc and Cl_2-GePc (Figure 1). Cl-AlPc has also been extensively studied in PHJ OPV applications. For example, Kim et al. fabricated both PHJ and BHJ devices containing Cl-AlPc and C_{60} and found that in both cases the resulting devices out performed comparable CuPc and C_{60} based devices.[15] It has also been demonstrated that Cl-AlPc can act as an electron acceptor when paired with pentacene.[65]

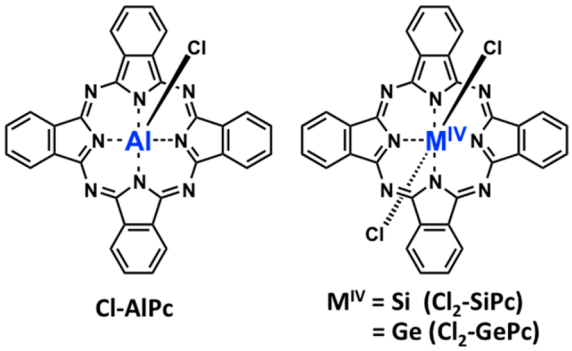

Figure 1. Chemical structure of chloro aluminum phthalocyanine (Cl-AlPc), dichloro silicon phthalocyanine (Cl_2-SiPc) and dichloro germanium phthalocyanine (Cl_2-GePc).

Cl-AlPc,[62] Cl_2-SiPc[57,58] and Cl_2-GePc[60,66] were synthesized according to methods presented in the literature, and purified by train sublimation prior to being integrated into devices.

All three phthalocyanine chlorides were first characterized by UV−vis spectroscopy. The resulting normalized absorption spectra for solutions in toluene as well as for vapor-deposited thin solid films are illustrated in Figure S1 and tabulated in Table 1. UV−vis spectroscopy was also performed in chloroform and dimethyl sulfoxide (DMSO) solution for comparison and the corresponding values can be found in Table S1. It is interesting to note is that with relatively similar film thicknesses, Cl-AlPc has a much broader absorption compared to the virtually identical absorption peaks associated with Cl_2-SiPc and Cl_2-GePc, which is not the case when in solution (Figure S1, Supporting Information). The optical band gap ($E_{Gap,Opt}$) was estimated from the onset of the absorbance data for Cl-AlPc, Cl_2-SiPc and Cl_2-GePc, and is tallied in Table 1. For example, Cl_2-SiPc and Cl_2-GePc were found to have an $E_{Gap,Opt}$ of 1.71 eV in solution and 1.55 eV in a thin solid film. Finally, when the optical absorptions for Cl-AlPc, Cl_2-SiPc and Cl_2-GePc were normalized for film thickness, it was noted that Cl_2-SiPc and Cl_2-GePc have a much higher absorption·nm^{-1} than Cl-AlPc (Figure S2, Supporting Information).

Cl-AlPc, Cl_2-SiPc and Cl_2-GePc were also electrochemically analyzed using cyclic voltammetry in dichloromethane solution with bis(pentamethyl cyclopentadienyl)iron internal standard. The resulting voltammograms are shown in Figure S3 (Supporting Information), and the relevant potentials are tabulated in Table S2 (Supporting Information). Although electrochemical analysis does give a good preliminary assessment of the energy levels of the frontier orbitals and the overall electrochemical behavior of a compound,[67] ultraviolet and X-ray photoelectron spectroscopy (UPS and XPS) are better used to accurately assess the highest occupied molecular orbital (HOMO) energy levels. UPS and XPS were therefore performed on Cl_2-SiPc and Cl_2-GePc thin films (and Cl-AlPc for reference). The resulting UPS spectra can be found in Figure S4 along with the obtained values in Table 1. The work functions obtained by XPS (Φ_{XPS}) are very similar to those obtained by UPS (Φ_{UPS}) and are very similar for all three Pcs, with values falling between 4.1 and 4.5 eV (Table 1). The ionization energy (IE) levels were calculated using UPS by adding the valence (HOMO) offset (Δe), ranging from 1.3 to 1.6 eV from the Fermi to Φ_{UPS}. Therefore, for all three metal halide Pcs the IE = 5.7 to 5.8 eV (Table 1). While there are no known UPS or XPS measurements of Cl_2-SiPC or Cl_2-GePc, for Cl-AlPc in all cases the reported values are within the differences of measured values.[68]

In general, the transport energy gap, $E_{Gap,T}$, is equal to the $E_{Gap,Opt}$ plus the energy associated with the exciton binding E_{Ex} ($E_{Gap,T} = E_{Gap,Opt} + E_{Ex}$).[69] Cho et al. identified that for Cl-AlPc (similar to CuPc) the $E_{Ex} \approx 0.24$ eV, which gives an $E_{Gap,T}$ of around 1.9 eV (when using $E_{Gap,Opt}$ = 1.66 eV).[68] Therefore, knowing the HOMO energy levels and the $E_{Gap,Opt}$ from the solid-state absorbance of these compounds, we then estimated the lowest unoccupied molecular orbital (LUMO) energy levels by using the $E_{Gap,T}$ and assuming E_{Ex} of Cl-AlPc ≈ 0.24 eV is similar for Cl_2-SiPc and Cl_2-GePc (Table 1).

Besides the basic electrophysical properties outlined above, when considering the application of a new compound as an organic electronic material, it is prudent to first examine its

DOI: 10.1021/am508491v
ACS Appl. Mater. Interfaces 2015, 7, 5076−5088

Table 1. UV−vis Absorbance and X-ray/Ultraviolet Photoelectron Spectroscopy Characterization Characteristics of Chloro Aluminum Phthalocyanine (Cl-AlPc), Dichloro Silicon Phthalocyanine (Cl_2-SiPc) and Dichloro Germanium Phthalocyanine (Cl_2-GePc) and Bis(pentafluoro phenoxy)silicon Phthalocyanine (F_{10}-SiPc)

	toluene		films							
sample	λ_{Max} [a] (nm)	$E_{Gap,OPT}$ [b] (eV)	λ_{Max} [a] (nm)	$E_{Gap,OPT}$ [b] (eV)	$E_{Gap,T}$ [c]	Φ_{XPS} [d] (eV)	Φ_{UPS} [d] (eV)	Δe (eV)	$IE_{,UPS}$ (eV)	E_{LUMO} [e] (eV)
Cl-AlPc	688	1.77	765	1.48	1.72	4.5	4.4	1.3	5.7	4.0
Cl_2-SiPc	685	1.77	752	1.56	1.80	4.1	4.1	1.6	5.7	3.9
Cl_2-GePc	691	1.76	750	1.56	1.80	4.5	4.4	1.4	5.8	4.0
F_{10}-SiPc	686	1.73	737	1.62	1.86	4.4	4.4	1.4	5.7	3.8

[a] λ_{Max} was determined as the peak wavelength of the absorbance spectra. [b] $E_{Gap,Opt}$ was determined from the onset of the absorbance spectra (Figure 6). [c] $E_{Gap,T} = E_{Gap,Opt} + E_{Ex}$,[69] where $E_{Ex} \approx 0.24$ eV.[68] [d] Work Function (Φ) determined by either X-ray photoelectron spectroscopy (XPS) and ultraviolet photoelectron spectroscopy (UPS). [e] Energy level associated with the lowest unoccupied molecular orbital (E_{LUMO}), was estimated using $E_{LUMO} = IE_{UPS} - E_{Gap,T}$.

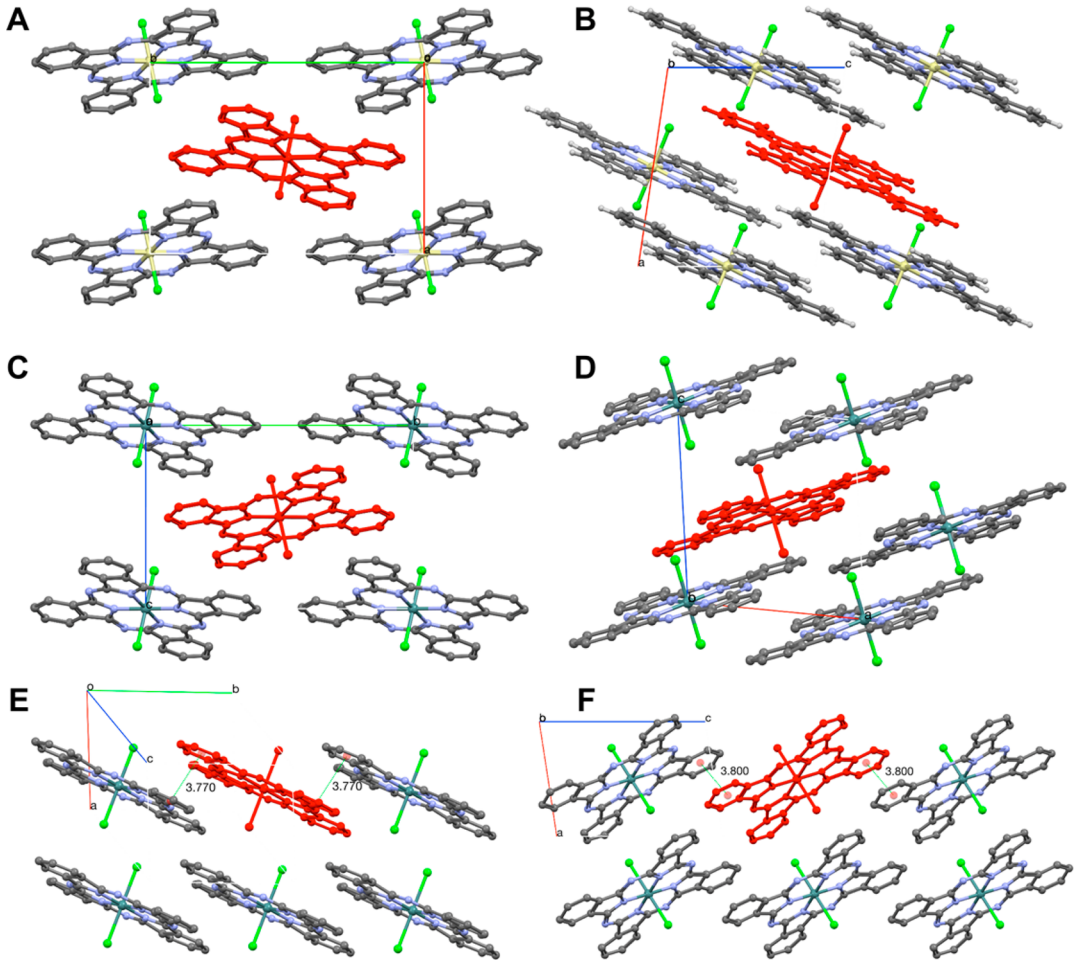

Figure 2. Solid-state arrangement of Cl_2-SiPc (A) and (B) (CCDC deposit #148330/identifier VIKVEQ, taken from Kojima et al.[56]) and confirmed by our group. Cl_2-GePc (C) and (D) (CCDC deposit ref #214379/identifier JAGWAQ, taken from Janczak and Kubiak[71]) and (E) and (F) Cl_2-GePc (CCDC deposit ref #214378/identifier JAGWAQ01, taken from Janczak and Kubiak[71]). The axes represent the unit cells.

solid-state arrangement (if available). When the published single crystal structure of Cl_2-SiPc (CCDC deposit #148330/identifier VIKVEQ, taken from Kojima et al.[56]) is examined, no significant $\pi-\pi$ interactions between Pc rings are apparent even though the molecules are relatively planar.[56] The shortest distance measured between the aromatic rings of the phthalocyanine units is 3.977 Å with a corresponding angle of 16.56° (Figure 2A,B). We also grew single crystals of Cl_2-SiPc by sublimation that were confirmed to be identical to that obtained by Kojima et al.[56] Silver et al. also reported a similar crystal structure of Cl_2-SiPc grown by solution; however, crystals grown by sublimation give a more accurate representation of the solid-state arrangement of molecules thermally evaporated into thin films and therefore this structure was not considered.[70]

Two crystal structures of Cl_2-GePc have been reported by Janczak and Kubiak.[71] Although the details of the synthesis of Cl_2-GePc and the subsequent growth of single crystals of two different polymorphs is not well detailed, an analysis of the P1 triclinic polymorph shows better three-dimensional $\pi-\pi$ interaction than Cl_2-SiPc at 3.770 and 3.800 Å and with the Pc chromophores nearly parallel (within error, Figure 2E,F).

DOI: 10.1021/am508491v
ACS Appl. Mater. Interfaces 2015, 7, 5076−5088

Scheme 1. Synthesis of Bis(pentafluoro phenoxy) Ailicon Phthalocyanine (F_{10}-SiPc) and Bis(pentafluoro phenoxy) Germanium Phthalocyanine (F_{10}-GePc) from Dichloro Silicon Phthalocyanine (Cl_2-SiPc) and Dichloro Germanium Phthalocyanine (Cl_2-GePc) and the Unexpected Formation of Difluoro Silicon Phthalocyanine (F_2-SiPc) and Difluoro Germanium Phthalocyanine (F_2-GePc), Respectively[a]

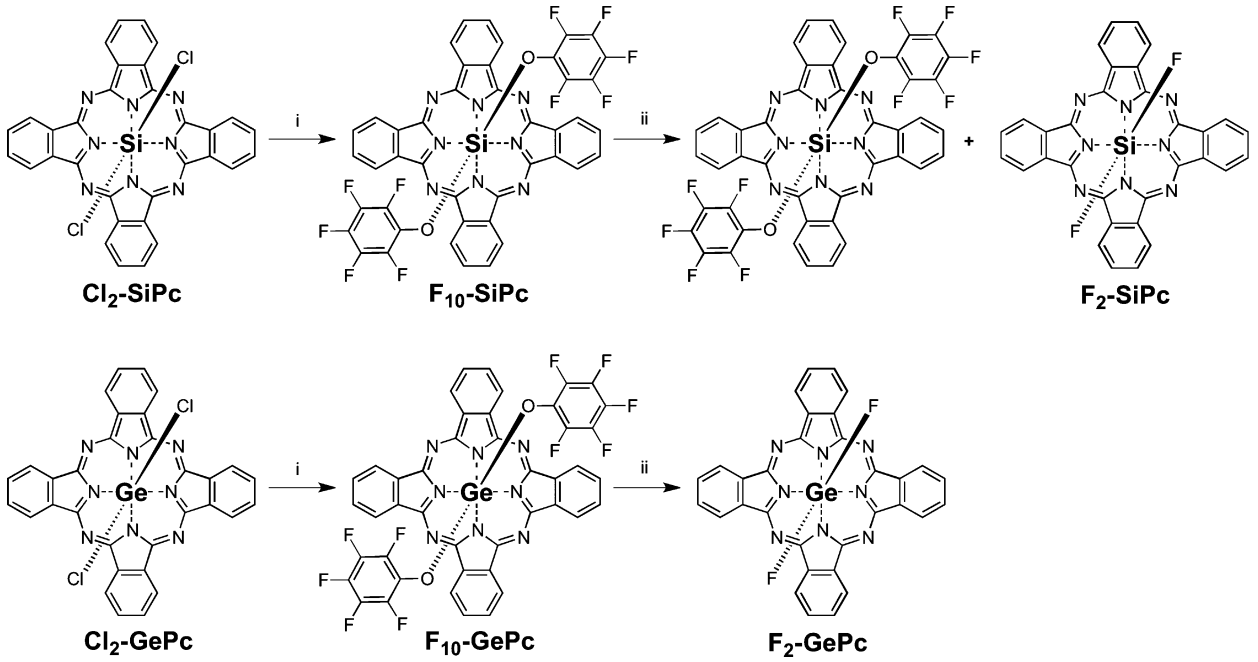

[a]Conditions: (i) 5:1 molar ratio of pentafluoro phenoxy to Cl_2-SiPc or Cl_2-GePc reflux in chlorobenzene overnight; (ii) under train sublimation conditions at 300−350 °C with the pressure at ~10^{-3} Torr.

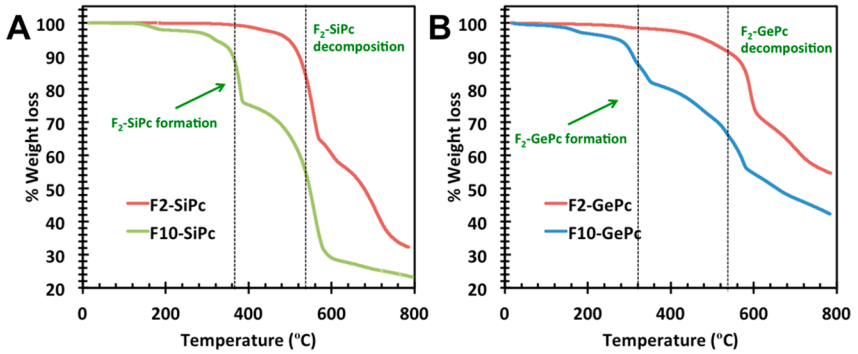

Figure 3. Thermogravimetric analysis (TGA) of (A) bis(pentafluoro phenoxy) silicon phthalocyanine (F_{10}-SiPcs) and difluoro silicon phthalocyanine (F_2-SiPc) and (B) bis(pentafluoro phenoxy) germanium phthalocyanine (F_{10}-GePcs) and difluoro germanium phthalocyanine (F_2-GePc).

The P21/n monoclinical polymorph of Cl_2-GePc is nearly identical in solid-state arrangement to Cl_2-SiPc, with no significant $\pi-\pi$ interactions (Figure 2C,D). These crystal structures suggest that Cl_2-GePc has potentially more favorable $\pi-\pi$ interaction compared to Cl_2-SiPc indicating that further investigation is merited and necessary (Figure 2E,F).

Our group has shown that in the case of boron subphthalocyanine (BsubPc), the addition of the pentafluoro phenoxy molecular fragment can reduce the sublimation temperature, significantly modify the electrochemical and optical properties and modify the solid-state arrangement.[44,45,72,73] Therefore, given the poor solid-state arrangements of Cl_2-SiPc and the P21/n monoclinic polymorph of Cl_2-GePc, we elected to see if taking an analogous pentafluoro phenoxylation approach with SiPc and GePc would yield similar results. We therefore synthesize F_{10}-GePc and F_{10}-SiPc by reacting Cl_2-SiPc or Cl_2-GePc each with a five molar excess of pentafluoro phenol in refluxing toluene (Scheme 1). Workup to obtain the crude product was relatively straightforward (see the Experimental Section).

Before fabrication of organic electronic devices, it is imperative that all organic compounds are purified to "electronic grade". In most cases, this level of purity is obtainable by train sublimation.[64] During train sublimation, the sample is heated under vacuum to the point where it sublimes into a flowing carrier gas and travels along a temperature gradient where it then deposits on a surface down tube.[64] As mentioned above, Cl_2-SiPc and Cl_2-GePc were easily purified using this technique. However, when train subliming F_{10}-SiPc at 350 °C and roughly 1−5 × 10^{-3} Torr under nitrogen gas flow, we determined that approximately 5−10% (estimated by mass spectrometry) of the sublimed product was difluoro silicon

DOI: 10.1021/am508491v
ACS Appl. Mater. Interfaces 2015, 7, 5076−5088

phthalocyanine (F_2-SiPc, Scheme 1) and roughly 20−25% (also estimated by mass spectrometry) of the material left in the sublimation boat was also F_2-SiPc. These results were consistent and reproducible and confirmed by elemental analysis (EA). When CO_2 was used as the train sublimation carrier gas, the amount of F_2-SiPc formation dropped to <1% (estimated by mass spectrometry).

To study this decomposition of F_{10}-SiPc and the formation of F_2-SiPc, we performed thermogravimetric analysis (TGA). To do this, a genuine sample of F_2-SiPc was synthesized (see the Experimental Section). The respective weight % relative to temperature (TGA) trace for F_{10}-SiPc and F_2-SiPc can be found in Figure 3. When the TGA trace for F_{10}-SiPc is analyzed, it is clear that two distinct transitions occur. The first drop in mass has a 5% weight loss onset at ∼370 °C resulting in a ultimate % mass loss of roughly 22 wt %, close to the molar mass difference between F_{10}-SiPc (906.72 g·mol^{-1}) and F_2-SiPc (568.61 g·mol^{-1}) of roughly 37 wt %. This temperature is slightly above the temperature employed during train sublimation. The second mass loss occurs at ∼540 °C, which is clearly the ultimate thermal decomposition. F_2-SiPc only shows one transition and it is at ∼540 °C, which is consistent with the decomposition temperature seen when F_{10}-SiPc is analyzed. This result indicates that the mass loss seen for F_{10}-SiPc at ∼370 °C is the formation of F_2-SiPc. Once formed, F_2-SiPc then ultimately decomposes at ∼540 °C. The mechanism by which this transformation to F_2-SiPc occurs is unclear; however, these results do suggest that if sublimation during device fabrication can be effected at a temperature of <370 °C then formation of F_2-SiPc can be avoided.

We also attempted to purify F_{10}-GePc using train sublimation with either N_2 or CO_2 as a carrier gas. In all attempts, temperatures in excess of 350 °C were necessary to see any mass movement and in all of our attempts 100% of F_{10}-GePc was converted to F_2-GePc (as determined by mass spectrometry). A genuine sample of F_2-GePc was also synthesized. When TGA analysis on F_{10}-GePc is performed, it becomes apparent that an initial mass loss, most likely a result of the F_2-GePc formation (by comparison against the TGA of the genuine sample) takes place at ∼330 °C followed by a second one at ∼500−540 °C (Figure 3B), which are at slightly lower temperatures than observed for F_{10}-SiPc (Figure 3A). Due to the elevated temperature required to sublime F_{10}-GePc, it was determined that the formation of F_2-GePc was unavoidable with our current purification setup and/or our current device fabrication apparatus. Given these observations, we did not continue the characterization of F_{10}-GePc.

X-ray photon electron spectroscopy (XPS) was performed on thermally evaporated films of F_{10}-SiPc and F_2-SiPc that were prepared under ultrahigh vacuum (∼10^{-10} Torr). Unfortunately, the sublimation rate of F_{10}-SiPc was only monitored by QCM and therefore the sublimation temperature itself was unknown. The resulting core level XPS can be found in Figure 4. As expected, when the peaks associated with the 1s orbital for oxygen (Figure 4B) are examined, it is clear that the film of F_2-SiPc shows no oxygen peak while that of F_{10}-SiPc has a clear peak at 532.5 eV. F_2-SiPc and F_{10}-SiPc both exhibit a similar single peak corresponding to the 1s orbital for silicon (Figure 4C) around 103 to 103.5 eV. However, when the 1s orbital for fluorine (Figure 4D) is examined, F_2-SiPc and F_{10}-SiPc exhibit clearly separate and distinct single peaks at 685.5 and 688.0 eV, respectively. The absence of a peak at 685.5 eV for the F_{10}-SiPc sample confirms that a vacuum deposition can be done without

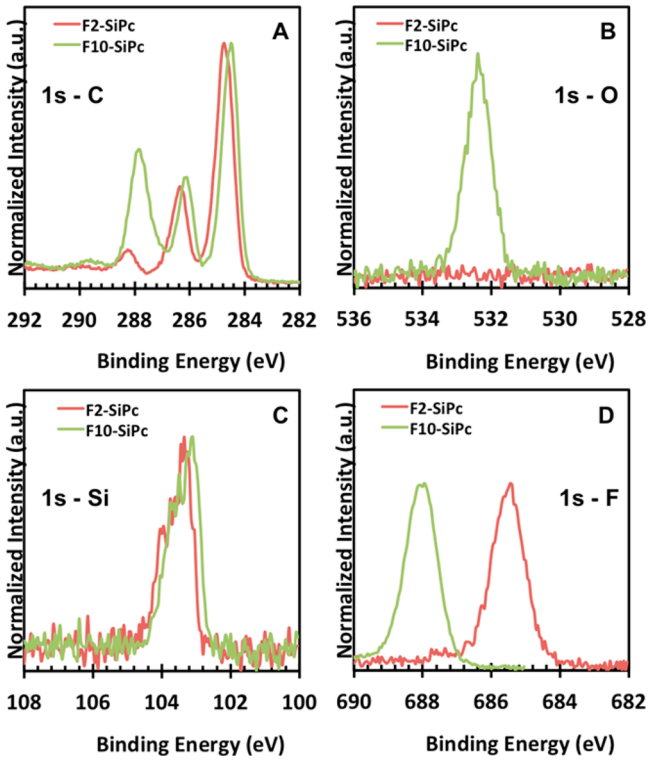

Figure 4. Core level X-ray photoelectron spectroscopy (XPS) of (A) 1s - carbon peak, (B) 1s oxygen peak (C) 1s - silicon peak and (D) 1s - fluorine peak for bis(pentafluoro phenoxy) silicon phthalocyanine (F_{10}-SiPcs) and difluoro silicon phthalocyanine (F_2-SiPc).

formation of F_2-SiPc. Although we are unsure of the actual deposition temperature, these results suggest that when the sublimation temperature is kept low (due to high operational vacuum, i.e. low pressure) the formation of F_2-SiPc can be avoided.

To further confirm this, we sublimed F_{10}-SiPc in the vacuum chamber that was used to fabricate F_{10}-SiPc containing PHJ OPV devices (see below for discussion on devices) at temperatures between 190 and 220 °C at a pressure of ∼1 × 10^{-7} Torr. Mass spectrometry confirmed that these films had no F_2-SiPc within them. Although we are confident no F_2-SiPc will be present in our PHJ OPV devices that are fabricated at ∼1 × 10^{-7} Torr, we do intend to further investigate the mechanism of its formation of F_2-SiPc on heating of F_{10}-SiPc.

Once synthesized and purified, single crystals of F_{10}-SiPc were grown. Single crystals that were grown by slow vapor diffusion of hexanes into a dichloromethane solution and heptane into a THF solution were found to be identical (CCD Deposition #1034275) and a benzene solvated crystal structure was also obtained from slow vapor diffusion of heptane into benzene (CCD Deposition #1034274) (detailed X-ray crystallography data can be found in the Supporting Information, Tables S3−S8 for nonsolvated and Tables S9−14 for solvated).

Figure 5 illustrates the solid-state arrangement within the F_{10}-SiPc crystals. As expected, the addition of a pentafluoro phenoxy fragment does enhance the $\pi-\pi$ interactions of the SiPc chromophores compared to Cl_2-SiPc. For instance, F_{10}-SiPc crystals have two of the peripheral aromatic groups of the SiPcs stacked in a parallel fashion, at a minimum distance of 3.654 Å with a corresponding maximum angle of 3.14° between the aromatic planes. In addition to the stacking of the Pc

DOI: 10.1021/am508491v
ACS Appl. Mater. Interfaces 2015, 7, 5076−5088

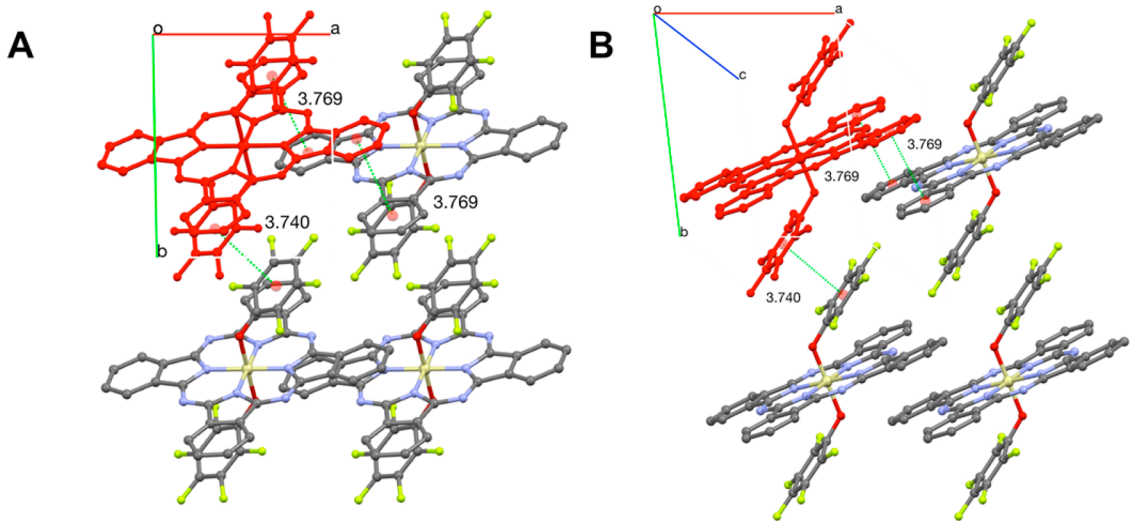

Figure 5. Solid-state arrangement of (A) face on view and (B) side view of F_{10}-SiPc obtained by single crystal X-ray diffraction (CCDC deposit #1034275). The dotted green lines represent molecular $\pi-\pi$ interactions between neighboring molecules (<then 3.8 Å). Identical single crystals were grown from slow vapor diffusion of hexanes into a dichloromethane solution or heptane into a THF solution. The axis represents the unit cell.

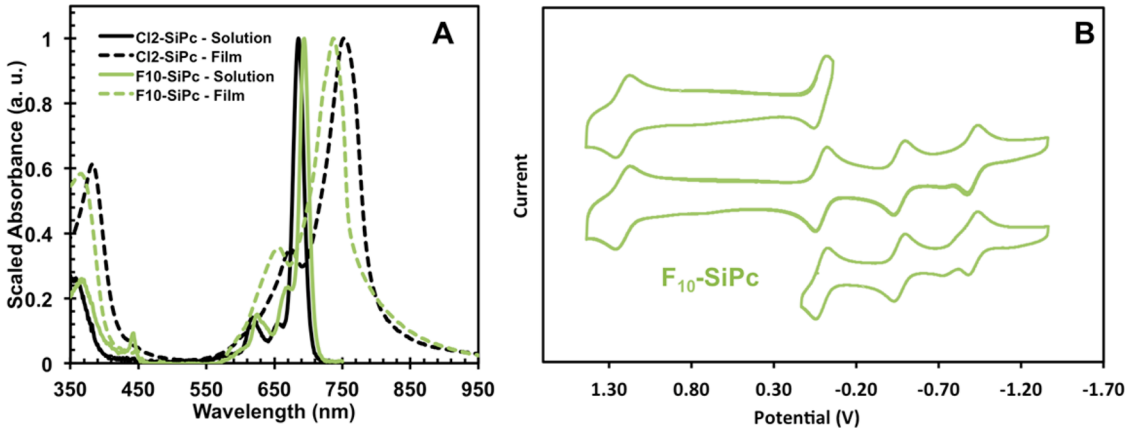

Figure 6. (A) Scaled UV−vis absorbance in toluene (solid lines) and as sublimed films (dashed lines) of Cl_2-SiPc and F_{10}-SiPc and (B) characteristic cyclic voltammograms of F_{10}-SiPc vs Ag/AgCl (dichloromethane; glass carbon working electrode; platinum wire counter electrode and an internal standard of bis(pentamethyl cyclopentadienyl) iron averaged over three runs using a scan rate of 100 mV/s).

peripherals, stacking of the pentafluoro phenoxy groups was also observed with a molecular distances of 3.740 Å with a corresponding angle of 0° between planes (parallel) (Figure 5B).

UV−vis spectroscopy was performed on F_{10}-SiPc in toluene solution as well as on 50−80 nm films obtained by thermal sublimation and compared against Cl_2-SiPc (Figure 6). The λ_{Max} of F_{10}-SiPc is $\lambda_{Max,\ Toluene}$ = 686 nm for toluene solution and $\lambda_{Max,\ Film}$ = 737 nm for the film (Figure 6A). These values are very similar to those obtained for the Cl_2-SiPc, where $\lambda_{Max,\ Toluene}$ = 685 nm in toluene solution and a $\lambda_{Max,\ Film}$ = 752 nm for the film (Table 1, Figure 6A). The $E_{Gap,\ Opt}$ was calculated from the solution spectra and from the solid-state spectra and is tabulated in Table 1. Despite slight changes in their respective absorbance, the addition of pentafluoro phenoxy groups has little effect on the overall shape of the absorbance or the band gap compared to Cl_2-SiPc. However, when normalized to film thickness (Figure S2, Supporting Information) the absorbance was roughly ≈10% greater for F_{10}-SiPc compared to Cl_2-SiPc, which is consistent with the ≈10% increase in solid-state density measured by X-ray crystallography (1.692 g·cm^{-3} for F_{10}-SiPc and 1.509 g·cm^{-3} for Cl_2-SiPc, Tables S3 and S8, Supporting Information).

Cyclic voltammetry (CV) was performed on F_{10}-SiPc (Figure 6B, Table S2, Supporting Information). Scanning at a positive potential reveals a completely reversible peak at +1.22 V whereas reductive scanning shows multiple completely reversible reductions at −0.46 and −0.91 V (Figure 6B, Table S2, Supporting Information). These values are very similar to those obtained for Cl_2-SiPc (Figure S3, Supporting Information) with the exception that the data is much clearer due to the higher solubility of F_{10}-SiPc in DCM. UPS and XPS were also performed on F_{10}-SiPc. The UPS spectra can be found in Figure S5 (Supporting Information) along with the obtained values in Table 1. The Φ_{XPS} and Φ_{UPS} as well as the IE of Cl_2-SiPc and F_{10}-SiPc were determined to be equivalent (Table 1). Finally, the LUMO level of F_{10}-SiPc was estimated and can be found in Table 1.

Photovoltaic Device Analysis. A series of planar heterojunciton (PHJ) OPV devices were fabricated containing Cl_2-SiPc, F_{10}-SiPc and Cl_2-GePc as active layers. Figure 7 illustrates the estimated energy levels used for PHJ OPV configurations as well as a visual representation of the device

DOI: 10.1021/am508491v
ACS Appl. Mater. Interfaces 2015, 7, 5076−5088

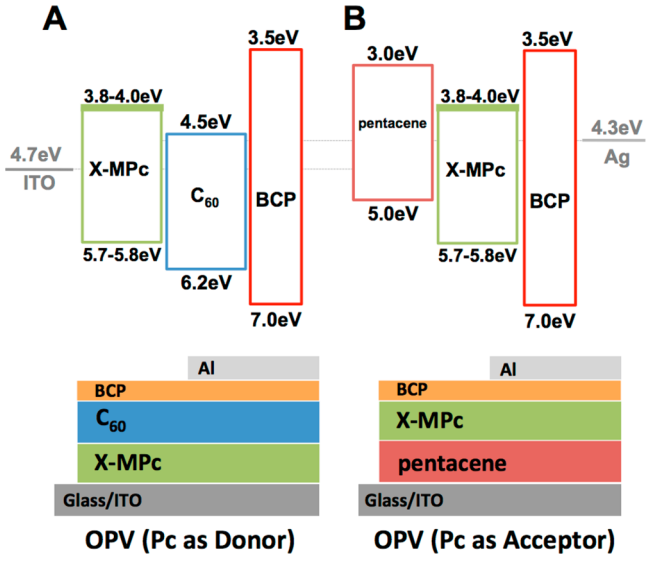

Figure 7. Estimated energy levels used for PHJ OPV configurations where X-MPc = Cl_2-GePc, Cl_2-AlPc, Cl_2-SiPc or F_{10}-SiPc are used as (A) the electron acceptor layer in a PHJ OPV device or B) the electron donor layer in a PHJ OPV device. The representative E_{HOMO} levels were either taken from the literature or determined by UPS (Table 1) and the E_{LUMO} levels were either taken from the literature or estimated from the difference between the E_{HOMO} and the $E_{Gap,T}$ the transfer energy gap (Table 1).

structures. To begin we assessed each as an electron donating materials paired with C_{60} as a standard electron acceptor material. As a point of comparison we also fabricated a series of baseline OPV devices using Cl-AlPc as the electron donor material. All devices had the structure: ITO/PEDOT:PSS/X-MPc(20 nm)/C_{60}(40 nm)/BCP(7.5 nm)/Ag. The resulting J–V curves and external quantum efficiency (EQE) versus wavelength plots are illustrated in Figure 8A,B, respectively.

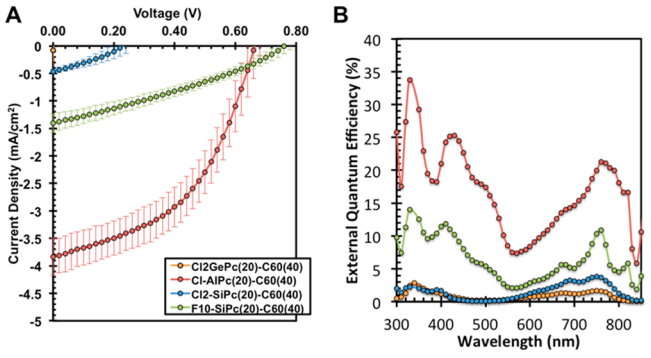

Figure 8. (A) J–V curves and (B) external quantum efficiency (% vs nm) for a series of X-MPc/C_{60} OPV devices. The legend in panel A is the same as for panel B.

On average, our Cl-AlPc/C_{60} PHJ baseline OPV devices were characterized as having a J_{SC} = 3.9 ± 0.3 mA·cm^{-2}, V_{OC} = 0.68 ± 0.03 V, FF = 0.48 ± 0.03 and η_p = 1.26 ± 0.2% (Table 2, Figure 8A). These metrics are in line with those reported by So et al.,[15] as are the EQE spectra. However, it should be noted that the devices of So et al. did not include a PEDOT:PSS injection layer. We found that when the PEDOT:PSS layer was not included for our setup a significant number of short circuited devices were obtained. This type of observation is not uncommon.[20]

Thereafter, PHJ OPV devices with 20 nm of Cl_2-SiPc (device B), 20 nm of F_{10}-SiPc (device C) or 20 nm of Cl_2-GePc were fabricated whereby the corresponding Pc was substituted for Cl-AlPc (Table 2, Figure 8). In the case of Cl_2-SiPc (device B, Table 2), a functional OPV device was obtained with the following metrics: V_{OC} = 0.24 ± 0.05; J_{SC} = 0.47 ± 0.05; FF = 0.32 ± 0.03; η_p = 0.04 ± 0.01. Although the resulting device characteristics were not as favorable as our baseline, they illustrate that Cl_2-SiPc can function as an electron donor material when paired with C_{60}. When the 20 nm of Cl_2-SiPc was replaced with 20 nm of F_{10}-SiPc (device C), the device experienced an improvement in both V_{OC} and J_{SC}. Device C was characterized by having a V_{OC} = 0.76 ± 0.03; J_{SC} = 1.4 ± 0.2; FF = 0.31 ± 0.005; η_p = 0.34 ± 0.04 (Figure 8, Table 2). Although these F_{10}-SiPc containing devices showed an improved V_{OC} relative to Cl-AlPc, the devices did not outperform the base device in terms of measured efficiency (Figure 8, Table 2). There is some evidence that the addition of shielding to the π-system can reduce parasitic carrier leakage and charge recombination at the donor/acceptor interface resulting in a significant increase in V_{OC}.[74−76] However, in these examples, the increase in V_{OC} is paired with a decrease in J_{SC}.[74−76] The pentafluoro phenoxylation of SiPc increased both the V_{OC} and J_{SC}, suggesting the improved solid-state arrangement of the SiPc, does play a significant role in the improved device performance and perhaps is not prone to decreasing the J_{SC}. It should again be noted that both F_{10}-SiPc and Cl_2-SiPc films were identified as having greater relative absorption to Cl-AlPc but a narrower absorption profile.

The incorporation of Cl_2-GePc (device J) resulted in a device with little to no diode character even when irradiated with the equivalent of 2 suns of simulated light (Figure 8, Table 2). A possible reason for this observation could be that we misidentified the peak in the UPS spectra of Cl_2-GePc (Figure S4, Supporting Information) corresponding to the HOMO energy level. On closer inspection of the UPS spectra of Cl_2-GePc, there is a very small broad peak centered at −0.6 eV. This peak is confirmed and is not present in the UPS spectrum of Cl-AlPc or Cl_2-SiPc. If this broad poorly defined peak is used to calculate the HOMO level of Cl_2-GePc, the result is an IE ≈ 4.8 eV. If this is accurate, then it could explain the poor to nonexistent PHJ OPV device characteristics as this HOMO level is approximately equivalent the LUMO level of C_{60}. Unfortunately, our electrochemical analysis cannot be used to confirm this hypothesis due to its relatively low quality. Further discussion on Cl_2-GePc and this idea appears below.

Based on the calculated HOMO and LUMO energy levels, it was apparent to us that Cl_2-SiPc, F_{10}-SiPc and Cl_2-GePc could also be applied as electron acceptors when paired with pentacene (Figure 7). Beaumont and Jones have recently determined that Cl-AlPc is a potential C_{60} replacement and a viable electron acceptor material in PHJ OPV devices.[65] Similarly, Jones et al. have shown the dual functionality of halo BsubPcs in OPV devices.[29] We have also shown that a BsubPc we refer to as pentafluoro phenoxy BsubPc (F_5-BsubPc) also has dual functionality and can be applied either as an electron donating or an electron accepting material in OPV devices.[23]

We therefore first fabricated a pentacene/C_{60} baseline PHJ OPV with a similar configuration to that reported by Sullivan et al.[77] except with PEDOT:PSS between the ITO and pentacene

DOI: 10.1021/am508491v
ACS Appl. Mater. Interfaces 2015, 7, 5076−5088

Table 2. Organic Photovoltaic (OPV) Device Structure and Characterization

device[a]	donor (nm)	acceptor (nm)	BCP (nm)	V_{OC}[b] (V)	J_{SC}[b] (mA·cm^{-2})	FF[b]	η_{power}[b] (%)
device A	Cl-AlPc(20)	C_{60}(40)	11.0	0.68 ± 0.03	3.9 ± 0.3	0.48 ± 0.03	1.26 ± 0.2
device B	Cl_2-SiPc(20)	C_{60}(40)	7.5	0.24 ± 0.05	0.47 ± 0.05	0.32 ± 0.03	0.04 ± 0.01
device C	F_{10}-SiPc(20)	C_{60}(40)	7.5	0.76 ± 0.03	1.4 ± 0.2	0.31 ± 0.01	0.34 ± 0.04
device D	pentacene(43)	C_{60}(40)	11.0	0.29 ± 0.02	7.0 ± 0.7	0.46 ± 0.05	0.95 ± 0.2
device E	pentacene(43)	Cl_2-SiPc(40)	11.0	0.14 ± 0.01	2.3 ± 0.3	0.35 ± 0.02	0.11 ± 0.02
device F	pentacene(43)	F_{10}-SiPc(40)	11.0	0.41 ± 0.01	2.4 ± 0.2	0.45 ± 0.02	0.45 ± 0.03
device G	α-6T (60)	Cl_2-SiPc(20)	7.5	0.29 ± 0.02	1.2 ± 0.1	0.39 ± 0.04	0.13 ± 0.02
device H	α-6T (60)	F_{10}-SiPc(20)	7.5	0.41 ± 0.02	2.7 ± 0.2	0.36 ± 0.01	0.40 ± 0.04
device I	pentacene(43)	Cl_2-GePc(40)	7.5	0.08 ± 0.008[c]	1.67 ± 0.07[c]	0.36 ± 0.05[c]	0.05 ± 0.01[c]
device J	Cl_2-GePc(20)	C_{60}(40)	7.5	0.02 ± 0.02[c]	0.1 ± 0.1[c]	–[c]	–[c]

[a]Device structure: ITO/PEDOT:PSS/donor(20, 43, or 60 nm)/acceptor(20 or 40 nm)/BCP(7.5 or 11.0 nm)/Ag(80 nm). [b]Device characteristics taken from an average of 6–10 pixels over 2–4 devices. [c]These PHJ OPV devices were tested at 2 suns.

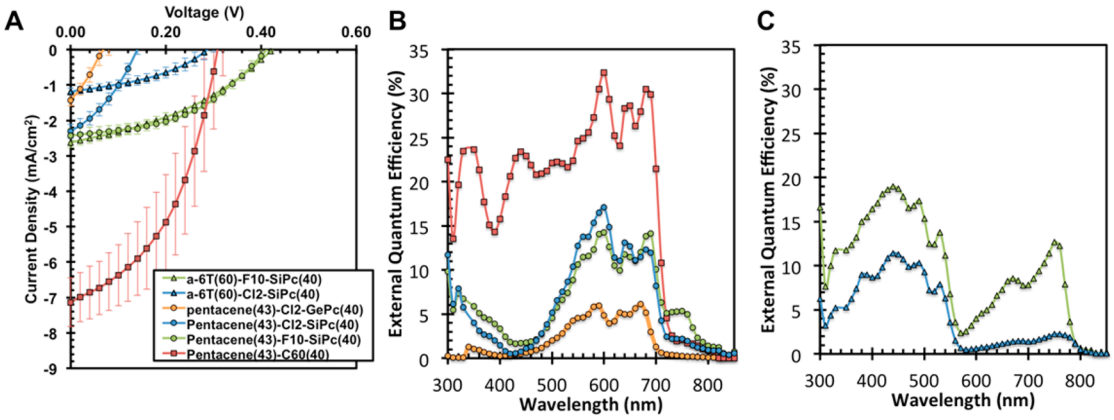

Figure 9. (A) *J*–*V* curves and (B, C) external quantum efficiency (% vs nm) for a series of pentacene/X-MPc and α-6T/SiPc OPV devices. The legend in panel A is the same as for panels B and C.

(to prevent shorted devices as mentioned above). We also used Ag instead of Al as the counter electrode. Our device configuration was ITO/PEDOT:PSS/pentacene(43 nm)/C_{60}(40 nm)/BCP(11 nm)/Ag. On average, our baseline PHJ OPV devices were characterized as having a J_{SC} = 7.0 ± 0.7 mA·cm^{-2}, V_{OC} = 0.29 ± 0.02 V, FF = 0.46 ± 0.05 and η_p = 0.95 ± 0.2%, which is similar to the characteristics from Sullivan et al., albeit with a poorer V_{OC} (J_{SC} = 6.70 mA·cm^{-2}, V_{OC} = 0.41 V, FF = 0.54 and η_p = 1.50%).[77]

Next we substituted Cl_2-SiPc, F_{10}-SiPc and Cl_2-GePc for C_{60} with the same device configuration: Cl_2-GePc (device I), Cl_2-SiPc (device E) and F_{10}-SiPc (device F) (Figure 9, Table 2). The devices containing Cl_2-SiPc (device E) exhibited a J_{SC} = 2.3 ± 0.3 mA·cm^{-2}, V_{OC} = 0.14 ± 0.01 V, FF = 0.35 ± 0.02 and η_p = 0.11 ± 0.02% whereas the use of F_{10}-SiPc (device F) exhibited a J_{SC} = 2.4 ± 0.2 mA·cm^{-2}, V_{OC} = 0.41 ± 0.01 V, FF = 0.45 ± 0.02 and η_p = 0.45 ± 0.03% (Table 2, Figure 9A). In the cases of F_{10}-SiPc and Cl_2-SiPc, two additional peaks in the EQE plot are present between 300 and 400 nm and between 700 and 800 nm, which correspond to the absorbance of the SiPc chromophore (Figure 9B). It is interesting to note that these peaks are more pronounced when using F_{10}-SiPc compared to Cl_2-SiPc, indicating a more significant photogeneration contribution from F_{10}-SiPc.

In contrast to its performance as an electron donating material, the PHJ OPV incorporating Cl_2-GePc as an electron acceptor material was functional albeit with dismal performance even when irradiated with the equivalent of 2 suns of simulated light. With such poor device performance, it is hard to offer an explanation of the root cause. However, if our hypothesis above is correct, that we have miscalculated the HOMO and LUMO energy levels of Cl_2-GePc, then the offset between the HOMO of pentacene and HOMO of Cl_2-GePc may only be ≥0.2 eV. This offset is known in some cases to be enough for a rectifying interfacing, but that is rare.[28,78]

Additionally, it has been recently shown that when properly engineered, pentacene and C_{60} containing devices can take advantage of triplet fission to reach quantum efficiencies exceeding 100%.[79] Very few examples of singlet fission capable materials are known in the literature,[80] and materials capable of harvesting these triplets are equally rare.[81,82] Recently, we have shown that hexachloro BsubPc chloride (Cl-Cl_6BsubPc) can harvest triplets from the singlet fission process within pentacene.[24] A large peak in the EQE spectrum between 600 and 700 nm can be used to identify the singlet fission process. This characteristic region of activity is present in the EQE plots for the pentacene/Cl_2-SiPc, pentacene/F_{10}-SiPc and pentacene/Cl_2-GePc devices (Figure 9B) suggesting that all Cl_X-MPcs in this study can extract the triplet energy resulting from the singlet fission process within pentacene. These results are consistent with the previous findings that electron acceptors with LUMO energies greater than 3.8 eV can effectively dissociate pentacene triplets.[81,82]

In order to avoid the singlet fission process, a 60 nm layer of α-sexithiophene (α-6T) was used as a donor layer and paired with either 40 nm of Cl_2-SiPc (device G) or F_{10}-SiPc (device H). The device containing Cl_2-SiPc (device G) exhibited a J_{SC} = 1.2 ± 0.1 mA·cm^{-2}, V_{OC} = 0.29 ± 0.02 V, FF = 0.39 ± 0.04 and

DOI: 10.1021/am508491v
ACS Appl. Mater. Interfaces 2015, 7, 5076–5088

η_P = 0.13 ± 0.02% whereas the use of F_{10}-SiPc (Device H) exhibited a J_{SC} = 2.7 ± 0.2 mA·cm^{-2}, V_{OC} = 0.41 ± 0.02 V, FF = 0.36 ± 0.01 and η_P = 0.40 ± 0.04% (Figure 9A). The EQE plots show two distinct contributions corresponding to the absorption of α-6T and X-MPc (Figure 9C). Compared to the baseline device, the use of F_{10}-SiPc resulted in an increased V_{OC} but an overall lower η_P due to a lower short circuit current density (J_{SC}). Regardless, these results indicate that both Cl_2-SiPc and F_{10}-SiPc can act as acceptor molecules when paired with either α-6T or pentacene, and that F_{10}-SiPc outperforms Cl_2-SiPc. Clearly, further device engineering and optimization is required to improve the J_{SC} and ultimate efficiency of PHJ OPVs based on the presented Pcs.

To summarize our findings, although our initial PHJ OPV devices containing either Cl_2-SiPc or F_{10}-SiPc do not surpass the device characteristics of our baseline devices, some conclusions can be drawn from this data. Due to the virtually identical opto-/electrophysical properties of Cl_2-SiPc and F_{10}-SiPc, and given we know their respective solid-state arrangements, the improved device performance of F_{10}-SiPc over Cl_2-SiPc can be attributed to the observed improved solid-state arrangement and the potential π-system shielding of F_{10}-SiPc compared to Cl_2-SiPc. Additionally, Cl_2-SiPc or F_{10}-SiPc can be applied as either an electron donor (when paired with C_{60}) or as an electron acceptor (when paired with pentacene or α-6T) in PHJ OPV devices.

The results of this study with respect to SiPc are clear; however, the results for Cl_2-GePc present a bit of a conundrum. To summarize, Cl_2-GePc has a generally good solid-state arrangement for a potential organic electronic material (Figure 2). When we paired Cl_2-GePc with C_{60} in a PHJ OPV, where its function would be as an electron donating material, the result was a nonfunctional device. In contrast, when Cl_2-GePc was paired with pentacene the device produced a photocurrent, albeit with no EQE contribution from Cl_2-GePc, suggesting that Cl_2-GePc did contribute to the movement of charge but not its photogeneration. With limited literature precedent for the use of Cl_2-GePc in modern organic electronic devices, it is hard to offer a concise hypothesis or a set of hypotheses that is consistent with these observations. However, given GePc derivatives at one time warranted patent protection and the favorable solid-state arrangement of Cl_2-GePc outlined above, we felt the poor functionality of Cl_2-GePc warranted further study. One hypothesis we did offer above was that a small broad peak in the UPS spectrum at ∼−0.6 eV could represent a more accurate estimation of the HOMO energy level of Cl_2-GePc. At this energy level, the HOMO and LUMO energy levels would be approximately equivalent to that of pentacene, therefore the pentacene/Cl_2-GePc would function more like a single junction device and could account for the lack of EQE contribution from Cl_2-GePc. This second estimation of the HOMO and LUMO energy levels is also in line with the observed nonfunctionality of the Cl_2-GePc/C_{60} device.

In an attempt to confirm the second estimated HOMO and LUMO energies of Cl_2-GePc, we paired Cl_2-GePc with our known electron accepting material F_5-BsubPc, (energy level diagram Figure S7, Supporting Information).[23] A series of Cl_2-GePc/F_5-BsubPc devices were fabricated, and the resulting device characteristics can be found in the Supporting Information (Figure S7). Although the resulting devices did exhibit diode-like behavior, they again had dismal device characteristics; the J_{SC} was below 0.05 mA·cm^{-2} and no photogeneration due to the Cl_2-GePc could be identified in the EQE plot (Figure S7A, Supporting Information). This final attempt leads us to the preliminary conclusion that perhaps Cl_2-GePc can be used in organic electronic devices where a potential is applied (for example, a photoreceptor as patented by Xerox Corporation[32−36]) but not in one where current production and extraction is required (OPV). Further study is required to solidify this hypothesis.

CONCLUSION

In conclusion, we have assessed the potential application of Cl_2-SiPc, F_{10}-SiPc and Cl_2-GePc in modern organic electronic devices. Initially, we have shown that Cl_2-SiPc and Cl_2-GePc have very similar physical and electronic properties relative to more widely studied Cl-AlPc. We have also shown that Cl_2-SiPc and F_{10}-SiPc can act as an electron-donating layer in an unoptimized PHJ OPV device when paired with C_{60} whereas PHJ OPV devices of Cl_2-GePc/C_{60} did not show any diode characteristics. We also paired pentacene with Cl_2-SiPc, F_{10}-SiPc and Cl_2-GePc and α-sexithiophene with Cl_2-SiPc and F_{10}-SiPc in PHJ OPV devices where the Pcs were applied as electron acceptor layers. Although our initial devices did not outperform our baseline devices, they did illustrate the potential for the dual use of Cl_2-SiPc and F_{10}-SiPc as an active material in PHJ OPV devices; either as an electron donor or as an electron acceptor. We have shown that these three Pcs enabled the harvesting of triplet energy resulting from singlet fission in pentacene when applied as electron accepting materials.

Our initial devices also showed that F_{10}-SiPc universally outperforms Cl_2-SiPc in either role within an OPV. In all cases, the use of F_{10}-SiPc instead of Cl_2-SiPc, resulted in as much as a 3-fold increase in both V_{OC} and J_{SC} and a resulting 8-fold increase in η_P. The relative performance improvement that comes from using F_{10}-SiPc over Cl_2-SiPc is attributed to the improved solid-state arrangement and π-system shielding of F_{10}-SiPc over Cl_2-SiPc.

As a cautionary note, when purifying F_{10}-SiPc by train sublimation, it was discovered that F_{10}-SiPc underwent a reaction which resulted in the formation of small amounts of F_2-SiPc. F_{10}-SiPc was then evaporated at different pressures (i.e., different temperatures) and the films were analyzed using mass spectrometry and XPS to identify whether F_2-SiPc was present. At greater vacuum (lower pressure) and lower temperatures, the formation of F_2-SiPc was completely suppressed and F_{10}-SiPc could be purified and incorporated into OPV devices.

UV−vis spectroscopy in both a solution and in the solid-state resulted in very similar absorbance profiles and $E_{Gap,Opt}$ for F_{10}-SiPc and Cl_2-SiPc. Electrochemistry of F_{10}-SiPc identified completely reversible and stable oxidative and reductive peaks, whereas UPS was used to determine that both F_{10}-SiPc and Cl_2-SiPc have ionization energies of 5.7 eV. The only major difference between the compounds was determined by studying single crystals of the corresponding compounds by X-ray crystallography. F_{10}-SiPc experienced significant $\pi-\pi$ interaction between the benzene rings of the planar SiPcs whereas Cl_2-SiPc experienced little to none. Therefore, it can be concluded that the addition of pentafluoro phenoxy groups on the SiPc molecule has little to no effect on the optophysical properties; however, it does modify the solid-state arrangement and provide π-shielding.

We also attempted to synthesized F_{10}-GePc; however, under train sublimation conditions, regardless of the type of the carrier gas employed, pressure or temperature, a 100%

DOI: 10.1021/am508491v
ACS Appl. Mater. Interfaces 2015, 7, 5076−5088

formation of F_2-GePc was observed. Therefore, further attempts to purify, characterize and incorporate F_{10}-GePc into OPV devices were not undertaken.

■ ASSOCIATED CONTENT

Supporting Information

UV−vis absorption of Cl-AlPc, Cl_2-SiPc, Cl_2-GePc and C_{60}, UV−vis absorption of Cl-AlPc, Cl_2-GePc, Cl_2-SiPc and F_{10}-SiPc as thin solid films from vacuum deposition, electrochemical analysis of Cl-AlPc, Cl_2-SiPc and Cl_2-GePc, ultraviolet photoelectron spectroscopy (UPS) He Iα ($h\nu$ = 21.22 eV) valence band spectra of Cl-AlPc, Cl_2-SiPc and Cl_2-GePc, ultraviolet photoelectron spectroscopy (UPS) He Iα ($h\nu$ = 21.22 eV) valence band spectra of F_{10}-SiPc, estimated energy levels where Cl_2-GePc and F_5-BsubPc in a PHJ OPV device, $J-V$ curves and external quantum efficiency (% vs nm) for a series of Cl_2-GePc/F_5-BsubPc OPVs, UV−vis absorbance characterization of the Cl-AlPc, Cl_2-SiPc and Cl_2-GePc, electrochemical characterization of the Cl-AlPc, Cl_2-SiPc, Cl_2-GePc and F_{10}-SiPc, crystal data and structure refinement for F_{10}-SiPc, atomic coordinates and equivalent isotropic displacement parameters for F_{10}-SiPc, bond lengths [≈] and angles [∞] for F_{10}-SiPc, anisotropic displacement parameters, hydrogen coordinates and isotropic displacement parameters for F_{10}-SiPc, torsion angles [∞] for F_{10}-SiPc, crystal data and structure refinement for F_{10}-SiPc solvate, atomic coordinates and equivalent isotropic displacement parameters for F_{10}-SiPc solvate, bond lengths [≈] and angles [∞] for F_{10}-SiPc solvate, anisotropic displacement parameters for F_{10}-SiPc solvate, hydrogen coordinates and isotropic displacement parameters for F_{10}-SiPc solvate and torsion angles [∞] for F10-SiPc solvate. This material is available free of charge via the Internet at http://pubs.acs.org.

■ AUTHOR INFORMATION

Corresponding Author

*T. P. Bender. E-mail: tim.bender@utoronto.ca.

Notes

The authors declare no competing financial interest.

■ ACKNOWLEDGMENTS

This work was supported by a Natural Sciences and Engineer Research Council (NSERC) Banting Post-Doctoral fellowship to BHL and a Discovery Grant to TPB. This work was also supported by an Ontario government Queen Elizabeth II Graduate Scholarships in Science and Technology (QEII-GSST) to RTW and DSJ. The authors would also like to acknowledge financial support from Saudi Basic Industries (SABIC).

■ REFERENCES

(1) Listigovers, N. A.; Allen, C. G.; Martin, T. I.; Hamer, G. K.; Hsiao, C. K.; Baranyi, G. Hydroxygallium Phthalocyanine Pigments with Block Copolymer Binders. U.S. Patent 5,521,043, May 28, 1996.
(2) Giambalvo, V. A.; Somerville, N. J. Phthalocyanine Pigment Compositions. U.S. Patent 2,526,345, October 17, 1950.
(3) Funatsu, T.; Inuzuka, Y.; Mishina, T.; Kitamura, K.; Chiba, A. Phthalocyanine Pigment Compositions. U.S. Patent 4,221,606, September 9, 1980.
(4) Alfred, S.; Summit, N. J. Phthalocyanine Pigments. U.S. Patent 2,861,005, November 18, 1958.
(5) Eastes, J. W.; Somerville, N. J. Preparation of Phthalocyanine Pigments. U.S. Patent 2,770,629, November 13, 1956.
(6) de la Torre, G.; Claessens, C. G.; Torres, T. S. Phthalocyanines: Old Dyes, New Materials. Putting Color in Nanotechnology. *Chem. Commun.* **2007**, 2000−2015.
(7) Roberts, M. E.; Sokolov, A. N.; Bao, Z. Material and Device Considerations for Organic Thin-Film Transistor Sensors. *J. Mater. Chem.* **2009**, *19*, 3351−3363.
(8) Tang, W. M.; Ng, W. T.; Greiner, M. T.; Qiu, J.; Helander, M. G.; Lu, Z.-H. Comparison of CuPc-based Organic Thin-Film Transistors Made by Different Dielectric Structures. *J. Vac. Sci. Technol., B: Nanotechnol. Microelectron.: Mater., Process., Meas., Phenom.* **2013**, *31*, 0122011−0122016.
(9) Li, X.; Jiang, Y.; Xie, G.; Tai, H.; Sun, P.; Zhang, B. Copper Phthalocyanine Thin Film Transistors for Hydrogen Sulfide Detection. *Sens. Actuators, B* **2013**, *176*, 1191−1196.
(10) Deng, Z.; Lu, Z.; Chen, Y.; Yin, Y.; Zou, Y.; Xiao, J.; Wang, Y. Aluminum Phthalocyanine Chloride as a Hole Injection Enhancer in Organic Light-Emitting Diodes. *Solid-State Electron.* **2013**, *89*, 22−25.
(11) Wang, H.; Ji, Z.; Liu, M.; Shang, L.; Liu, G.; Liu, X.; Liu, J.; Peng, Y. Advances in Organic Field-Effect Transistors and Integrated Circuits. *Sci. China Ser. E: Technol. Sci.* **2009**, *52*, 3105−3116.
(12) Hou, J.; Guo, X. Active Layer Materials for Organic Solar Cells. In *Organic Solar Cells*; Green Energy and Technology; Springer London: London, 2012; pp 17−42.
(13) Chen, Y.-C.; Hsu, C.-Y.; Lin, R. Y.-Y.; Ho, K.-C.; Lin, J. T. Materials for the Active Layer of Organic Photovoltaics: Ternary Solar Cell Approach. *ChemSusChem* **2013**, *6*, 20−35.
(14) Xue, J.; Uchida, S.; Rand, B.; Forrest, S. 4.2% Efficient Organic Photovoltaic Cells with Low Series Resistances. *Appl. Phys. Lett.* **2004**, *84*, 3013−3015.
(15) Kim, D. Y.; So, F.; Gao, Y. Aluminum Phthalocyanine Chloride/C_{60} Organic Photovoltaic Cells with High Open-Circuit Voltages. *Sol. Energy Mater. Sol. Cells* **2009**, *93*, 1688−1691.
(16) Shaymurat, T.; Tang, Q.; Tong, Y.; Dong, L.; Liu, Y. Gas Dielectric Transistor of CuPc Single Crystalline Nanowire for SO_2 Detection Down to Sub-ppm Levels at Room Temperature. *Adv. Mater.* **2013**, *25*, 2269−2273.
(17) Zhou, Y.; Taima, T.; Miyadera, T.; Yamanari, T.; Kitamura, M.; Nakatsu, K.; Yoshida, Y. Phase Separation of Co-evaporated ZnPc:C_{60} Blend Film for Highly Efficient Organic Photovoltaics. *Appl. Phys. Lett.* **2012**, *100*, 233302.
(18) Jin, F.; Chu, B.; Li, W.; Su, Z.; Zhao, B.; Zhang, T.; Yan, X. The Influence of Donor Material on Achieving High Photovoltaic Response for Organic Bulk Heterojunction Cells with Small Ratio Donor Component. *Org. Electron.* **2013**, *14*, 1130−1135.
(19) Yuen, A. P.; Jovanovic, S. M.; Hor, A.-M.; Klenkler, R. A.; Devenyi, G. A.; Loutfy, R. O.; Preston, J. S. Photovoltaic Properties of M-Phthalocyanine/Fullerene Organic Solar Cells. *Sol. Energy* **2012**, *86*, 1683−1688.
(20) Chauhan, K. V.; Sullivan, P.; Yang, J. L.; Jones, T. S. Efficient Organic Photovoltaic Cells Through Structural Modification of Chloroaluminum Phthalocyanine/Fullerene Heterojunctions. *J. Phys. Chem. C* **2010**, *114*, 3304−3308.
(21) Williams, G.; Sutty, S.; Klenkler, R.; Aziz, H. Renewed Interest in Metal Phthalocyanine Donors for Small Molecule Organic Solar Cells. *Sol. Energy Mater. Sol. Cells* **2014**, *124*, 217−226.
(22) Yuen, A. P.; Bamsey, N. M.; Hor, A.-M.; Preston, J. S.; Klenkler, R. A.; Jovanovic, S. M.; Loutfy, R. O. Rubrene as an Additive in M-Phthalocyanine/Fullerene Organic Solar Cells. *Sol. Energy Mater. Sol. Cells* **2011**, *95*, 3137−3141.
(23) Morse, G. E.; Gantz, J. L.; Steirer, K. X.; Armstrong, N. R.; Bender, T. P. Pentafluorophenoxy Boron Subphthalocyanine (F5BsubPc) as a Multifunctional Material for Organic Photovoltaics. *ACS Appl. Mater. Interfaces* **2013**, *6*, 1515−1524.
(24) Beaumont, N.; Castrucci, J. S.; Sullivan, P.; Morse, G. E.; Paton, A. S.; Lu, Z.-H.; Bender, T. P.; Jones, T. S. Acceptor Properties of Boron Subphthalocyanines in Fullerene Free Photovoltaics. *J. Phys. Chem. C* **2014**, *118*, 14813−14823.
(25) Cnops, K.; Rand, B. P.; Cheyns, D.; Verreet, B.; Empl, M. A.; Heremans, P. 8.4% Efficient Fullerene-Free Organic Solar Cells

DOI: 10.1021/am508491v
ACS Appl. Mater. Interfaces 2015, 7, 5076−5088

Exploiting Long-Range Exciton Energy Transfer. *Nat. Commun.* **2014**, *5*, 1−6.
(26) Verreet, B.; Cnops, K.; Cheyns, D.; Heremans, P.; Stesmans, A.; Zango, G.; Claessens, C. G.; Torres, T.; Rand, B. P. Decreased Recombination Through the Use of a Non-fullerene Acceptor in a 6.4% Efficient Organic Planar Heterojunction Solar Cell. *Adv. Energy Mater.* **2014**, *4*, 1301413.
(27) Gommans, H.; Aernouts, T.; Verreet, B.; Heremans, P.; Medina, A.; Claessens, C. G.; Torres, T. Perfluorinated Subphthalocyanine as a New Acceptor Material in a Small-Molecule Bilayer Organic Solar Cell. *Adv. Funct. Mater.* **2009**, *19*, 3435−3439.
(28) Verreet, B.; Rand, B. P.; Cheyns, D.; Hadipour, A.; Aernouts, T.; Heremans, P.; Medina, A.; Claessens, C. G.; Torres, T. A 4% Efficient Organic Solar Cell Using a Fluorinated Fused Subphthalocyanine Dimer as an Electron Acceptor. *Adv. Energy Mater.* **2011**, *1*, 565−568.
(29) Beaumont, N.; Cho, S. W.; Sullivan, P.; Newby, D.; Smith, K. E.; Jones, T. S. Boron Subphthalocyanine Chloride as an Electron Acceptor for High-Voltage Fullerene-Free Organic Photovoltaics. *Adv. Funct. Mater.* **2011**, *22*, 561−566.
(30) Morse, G. E.; Bender, T. P. Boronsubphthalocyanines as Organic Electronic Materials. *ACS Appl. Mater. Interfaces* **2012**, *4*, 5055−5068.
(31) Branston, R.; Duff, J.; Hsiao, C. K.; Loutfy, R. O. *Photovoltaic Properties of Organic Photoactive Particle Dispersions: Polymeric Phthalocyanines*; ACS Symposium Series; American Chemical Society: Washington, DC, 1983; Vol. *220*, pp 437−455.
(32) Ong, B. S.; Bluhm, T. L.; Hsiao, C. K.; Duff, J. M. Hydroxygermanium Phthalocyanine Processes. U.S. Patent 5,382,493, January 17, 1995.
(33) Ong, B. S.; Hsiao, C. K. Photoconductive Imaging Members with Acetoxymetal Phthalocyanines. U.S. Patent 5,441,837, August 15, 1995.
(34) Ong, B. S.; Hsiao, C. K. Preparative Processes for Dihydroxygermanium Phthalocyanine. U.S. Patent 5,491,228, February 13, 1996.
(35) Branston, R. E.; Duff, J. M. Photoresponsive Imaging Members with Dihydroxy Metal Phthalocyanine Compositions. U.S. Patent 4,557,989, December 10, 1985.
(36) Borsenberger, P. M. *Organic Photoreceptors for Xerography*; Borsenberger, P. M., Ed.; CRC Press: Boca Raton, FL, 1998; Vol. *59*.
(37) Lim, B.; Margulis, G. Y.; Yum, J.-H.; Unger, E. L.; Hardin, B. E.; Graetzel, M.; McGehee, M. D.; Sellinger, A. Silicon-Naphthalo/Phthalocyanine-Hybrid Sensitizer for Efficient Red Response in Dye-Sensitized Solar Cells. *Org. Lett.* **2013**, *15*, 784−787.
(38) Honda, S.; Ohkita, H.; Benten, H.; Ito, S. Multi-colored Dye Sensitization of Polymer/Fullerene Bulk Heterojunction Solar Cells. *Chem. Commun.* **2010**, *46*, 6596−6598.
(39) Honda, S.; Nogami, T.; Ohkita, H.; Benten, H.; Ito, S. Improvement of the Light-Harvesting Efficiency in Polymer/Fullerene Bulk Heterojunction Solar Cells by Interfacial Dye Modification. *ACS Appl. Mater. Interfaces* **2009**, *1*, 804−810.
(40) Lessard, B. H.; Dang, J. D.; Grant, T. M.; Gao, D.; Seferos, D. S.; Bender, T. P. Bis(Tri-N-Hexylsilyl Oxide) Silicon Phthalocyanine: A Unique Additive in Ternary Bulk Heterojunction Organic Photovoltaic Devices. *ACS Appl. Mater. Interfaces* **2014**, *6*, 15040−15051.
(41) Anthony, J. E.; Brooks, J. S.; Eaton, D. L.; Parkin, S. R. Functionalized Pentacene: Improved Electronic Properties From Control of Solid-State Order. *J. Am. Chem. Soc.* **2001**, *123*, 9482−9483.
(42) Anthony, J. E.; Eaton, D. L.; Parkin, S. R. A Road Map to Stable, Soluble, Easily Crystallized Pentacene Derivatives. *Org. Lett.* **2002**, *4*, 15−18.
(43) Payne, M. M.; Parkin, S. R.; Anthony, J. E.; Kuo, C.-C.; Jackson, T. N. Organic Field-Effect Transistors From Solution-Deposited Functionalized Acenes with Mobilities as High as 1 $cm^2/V{\cdot}s$. *J. Am. Chem. Soc.* **2005**, *127*, 4986−4987.
(44) Castrucci, J. S.; Helander, M. G.; Morse, G. E.; Lu, Z.-H.; Yip, C. M.; Bender, T. P. Charge Carrier Mobility in Fluorinated Phenoxy Boron Subphthalocyanines: Role of Solid State Packing. *Cryst. Growth Des.* **2012**, *12*, 1095−1100.
(45) Morse, G. E.; Helander, M. G.; Maka, J. F.; Lu, Z.-H.; Bender, T. P. Fluorinated Phenoxy Boron Subphthalocyanines in Organic Light-Emitting Diodes. *ACS Appl. Mater. Interfaces* **2010**, *2*, 1934−1944.
(46) Wheeler, B. L.; Nagasubramanian, G.; Bard, A. J.; Schechtman, L. A.; Kenney, M. E. A Silicon Phthalocyanine and a Silicon Naphthalocyanine: Synthesis, Electrochemistry, and Electrogenerated Chemiluminescence. *J. Am. Chem. Soc.* **1984**, *106*, 7404−7410.
(47) Choi, M. T. M.; Choi, C.-F.; Ng, D. K. P. Assembling Tetrapyrrole Derivatives through Axial Coordination. *Tetrahedron* **2004**, *60*, 6889−6894.
(48) Cissell, J. A.; Vaid, T. P.; DiPasquale, A. G.; Rheingold, A. L. Germanium Phthalocyanine, GePc, and the Reduced Complexes SiPc(Pyridine)(2) and GePc(Pyridine)(2) Containing Antiaromatic pi-Electron Circuits. *Inorg. Chem.* **2007**, *46*, 7713−7715.
(49) Leng, X.; Ng, D. K. P. Axial Coordination of Porphyrinatocobalt(II) Complexes with Bis(pyridinolato)silicon(IV) Phthalocyanines. *Eur. J. Inorg. Chem.* **2007**, *2007*, 4615−4620.
(50) Kwag, G.; Bae, C.; Kim, S.; Lee, J.-J.; Kenney, M. E. Electronic Property of Group IV Phthalocyanine Dimers: SiPcMPc. *Inorg. Chim. Acta* **2009**, *362*, 2027−2032.
(51) Brewis, M.; Clarkson, G. J.; Goddard, V. Silicon Phthalocyanines with Axial Dendritic Substituents. *Angew. Chem., Int. Ed.* **1998**, *37*, 1092−1094.
(52) Brewis, M.; Helliwell, M.; McKeown, N. B.; Reynolds, S.; Shawcross, A. Phthalocyanine-Centred Aryl Ether Dendrimers with Oligo(Ethyleneoxy) Surface Groups. *Tetrahedron Lett.* **2001**, *42*, 813−816.
(53) Brewis, M.; Helliwell, M.; McKeown, N. B. Phthalocyanine-Centred and Naphthalocyanine-Centred Aryl Ether Dendrimers with Oligo(ethyleneoxy) Surface Groups. *Tetrahedron* **2003**, 3863−387259.
(54) Barker, C. A.; Findlay, K. S.; Bettington, S.; Batsanov, A. S. Synthesis of New Axially-Disubstituted Silicon-Phthalocyanine Derivatives: Optical and Structural Characterisation. *Tetrahedron* **2006**, *62*, 9433−9439.
(55) MartÌn-Gomis, L.; Ohkubo, K.; Fernández-Lázaro, F.; Fukuzumi, S.; Sastre-Santos, Á. Synthesis and Photophysical Studies of a New Nonaggregated C_{60}−Silicon Phthalocyanine−C_{60}Triad. *Org. Lett.* **2007**, *9*, 3441−3444.
(56) Kojima, Y.; Osano, Y. T.; Ohashi, T. X-ray Crystal Structure Analysis of Silicon Phthalocyanines. Study of the Relationship between Intermolecular Interaction and Photochemical Sensitivity. *Bull. Chem. Soc. Jpn.* **2000**, *73*, 2469−2475.
(57) Dahlen, M. A. The Phthalocyanines A New Class of Synthetic Pigments and Dyes. *Ind. Eng. Chem.* **1939**, *31*, 839−847.
(58) Lowery, M. K.; Starshak, A. J.; Esposito, J. N.; Krueger, P. C.; Kenney, M. E. Dichloro(Phthalocyanino)Silicon. *Inorg. Chem.* **1965**, *4*, 128−128.
(59) Claessens, C. G.; Hahn, U.; Torres, T. Phthalocyanines: From Outstanding Electronic Properties to Emerging Applications. *Chem. Rec* **2008**, *8*, 75−97.
(60) Joyner, R. D.; Kenney, M. E. Germanium Phthalocyanines. *J. Am. Chem. Soc.* **1960**, *82*, 5790−5791.
(61) de la Torre, G.; Vazquez, P.; Agullo-Lopez, F.; Torres, T. Phthalocyanines and Related Compounds: Organic Targets for Nonlinear Optical Applications. *J. Mater. Chem.* **1998**, *8*, 1671−1683.
(62) Guay, D.; Dodelet, J. P.; Cote, R.; Langford, C. H.; Gravel, D. Photoelectrochemistry of Some Aluminum Phthalocyanines in Regenerative Solar Cells. *J. Electrochem. Soc.* **1989**, *136*, 2272−2280.
(63) Fleetham, T. B.; Bakkan, N.; Mudrick, J. P.; Myers, J. D.; Cassidy, V. D.; Cui, J.; Xue, J.; Li, J. Enhanced Open-Circuit Voltage in Organic Photovoltaic Cells with Partially Chlorinated Zinc Phthalocyanine. *J. Mater. Sci.* **2013**, *48*, 7104−7114.
(64) Helander, M. G.; Morse, G. E.; Qiu, J.; Castrucci, J. S.; Bender, T. P.; Lu, Z.-H. Pentafluorophenoxy Boron Subphthalocyanine as a Fluorescent Dopant Emitter in Organic Light Emitting Diodes. *ACS Appl. Mater. Interfaces* **2010**, *2*, 3147−3152.
(65) Beaumont, N. L. Investigating New Materials and Understanding the Ambipolar Qualities of Organic Small Molecules for Use

DOI: 10.1021/am508491v
ACS Appl. Mater. Interfaces 2015, 7, 5076−5088

in Organic Photovoltaics. Ph.D. Thesis, The University of Warwick, Coventry, U. K., 2013.
(66) Joyner, R. D.; Linck, R. G.; Esposito, J. N.; Kenney, M. E. Dichloro- and Siloxygermanium Phthalocyanines. *J. Inorg. Nucl. Chem.* **1962**, *24*, 299−302.
(67) D'Andrede; Datta, S.; Forrest, S.; Djurovich, P.; Polikarpov, E.; Thompson, M. Relationship between the Ionization and Oxidation Potentials of Molecular Organic Semiconductors. *Org. Electron.* **2005**, *6*, 11−20.
(68) Cho, S. W.; Piper, L. F. J.; DeMasi, A.; Preston, A. R. H.; Smith, K. E.; Chauhan, K. V.; Sullivan, P.; Hatton, R. A.; Jones, T. S. Electronic Structure of C_{60}/Phthalocyanine/ITO Interfaces Studied Using Soft X-ray Spectroscopies. *J. Phys. Chem. C* **2010**, *114*, 1928−1933.
(69) Hill, I. G.; Kahn, A.; Soos, Z. G.; Pascal, R. A., Jr. Charge-Separation Energy in Films of Π-Conjugated Organic Molecules. *Chem. Phys. Lett.* **2000**, *327*, 181−188.
(70) Silver, J.; Frampton, C. S.; Fern, G. R.; Davies, D. A.; Miller, J. R.; Sosa-Sanchez, J. L. Novel Seven Coordination Geometry of Sn(IV): Crystal Structures of Phthalocyaninato Bis-(undecylcarboxylato)Sn(IV), Its Si(IV) Analogue, and Phthalocyaninato Bis(chloro)silicon(IV). The Electrochemistry of the Si(IV) Analogue and Related Compounds. *Inorg. Chem.* **2001**, *40*, 5434−5439.
(71) Janczak, J.; Kubiak, R. Two Isomorphous Complexes: Dichloro[phthalocyaninato(2-)]tin(IV) and Dichloro-[phthalocyaninato(2-)]germanium(IV). *Acta Crystallogr., Sect. C: Cryst. Struct. Commun.* **2003**, *59*, m237−m240.
(72) Morse, G. E.; Helander, M. G.; Stanwick, J.; Sauks, J. M.; Paton, A. S.; Lu, Z.-H.; Bender, T. P. Experimentally Validated Model for the Prediction of the HOMO and LUMO Energy Levels of Boronsubphthalocyanines. *J. Phys. Chem. C* **2011**, *115*, 11709−11718.
(73) Morse, G. E.; Gong, I.; Kawar, Y.; Lough, A. J.; Bender, T. P. Crystal and Solid-State Arrangement Trends of Halogenated Boron Subphthalocyanines. *Cryst. Growth Des.* **2014**, *14*, 2138−2147.
(74) Yang, L.; Zhou, H.; You, W. Quantitatively Analyzing the Influence of Side Chains on Photovoltaic Properties of Polymer-Fullerene Solar Cells. *J. Phys. Chem. C* **2010**, *114*, 16793−16800.
(75) Erwin, P.; Thompson, M. E. Elucidating the Interplay between Dark Current Coupling and Open Circuit Voltage in Organic Photovoltaics. *Appl. Phys. Lett.* **2011**, *98*, 223305.
(76) Schlenker, C. W.; Barlier, V. S.; Chin, S. W.; Whited, M. T.; McAnally, R. E.; Forrest, S. R.; Thompson, M. E. Cascade Organic Solar Cells. *Chem. Mater.* **2011**, *23*, 4132−4140.
(77) Sullivan, P.; Jones, T. S. Pentacene/Fullerene C_{60} Heterojunction Solar Cells: Device Performance and Degradation Mechanisms. *Org. Electron.* **2008**, *9*, 656−660.
(78) Sullivan, P.; Duraud, A.; Hancox, I.; Beaumont, N.; Mirri, G.; Tucker, J. H. R.; Hatton, R. A.; Shipman, M.; Jones, T. S. Halogenated Boron Subphthalocyanines as Light Harvesting Electron Acceptors in Organic Photovoltaics. *Adv. Energy Mater.* **2011**, *1*, 352−355.
(79) Congreve, D. N.; Lee, J.; Thompson, N. J.; Hontz, E.; Yost, S. R. External Quantum Efficiency Above 100% in a Singlet-Exciton-Fission-based Organic Photovoltaic Cell. *Science* **2013**, *340*, 334−340.
(80) Smith, M. B.; Michl, J. Recent Advances in Singlet Fission. *Annu. Rev. Phys. Chem.* **2013**, *64*, 361−386.
(81) Ehrler, B.; Walker, B. J.; Boehm, M. L.; Wilson, M. W. B.; Vaynzof, Y.; Friend, R. H.; Greenham, N. C. In Situ Measurement of Exciton Energy in Hybrid Singlet-Fission Solar Cells. *Nat. Commun.* **2012**, *3*, 1−6.
(82) Jadhav, P. J.; Brown, P. R.; Thompson, N.; Wunsch, B.; Mohanty, A.; Yost, S. R.; Hontz, E.; Van Voorhis, T.; Bawendi, M. G.; Bulovic, V.; Baldo, M. A. Triplet Exciton Dissociation in Singlet Exciton Fission Photovoltaics. *Adv. Mater.* **2012**, *24*, 6169−6174.

DOI: 10.1021/am508491v
ACS Appl. Mater. Interfaces 2015, 7, 5076−5088